Investigation of the energy leakage of showers from high energetic electrons in the forward calorimeter

Vladimir Drugakov

Report for work as guest scientist in DESY Zeuthen from 19.11 to 22.12.2001

Abstract

The leakage of electromagnetic showers in the forward calorimeter LCAL is studied. Simulations are made for several angles between 5 and 28 mrad and for energies of 100, 300 and 500 GeV. Two detector types are studied: a homogeneous $PbWO_4$ calorimeter and a diamond-tungsten sampling calorimeter. The strong leakage near the outer radius of the calorimeter can be cured by enlarging the size.

1 Introduction

1.1 TESLA

TESLA (TeV-Energy Superconducting Linear Accelerator) is a superconducting e^+e^- collider of initially 500 GeV total energy, extendable to 800 GeV, proposed by the DESY laboratory. The accelerator is foreseen to be constructed starting from the DESY site in Hamburg in north-west direction. The total length will be 33 km. A sketch of the TESLA linear collider is shown in Figure 1.

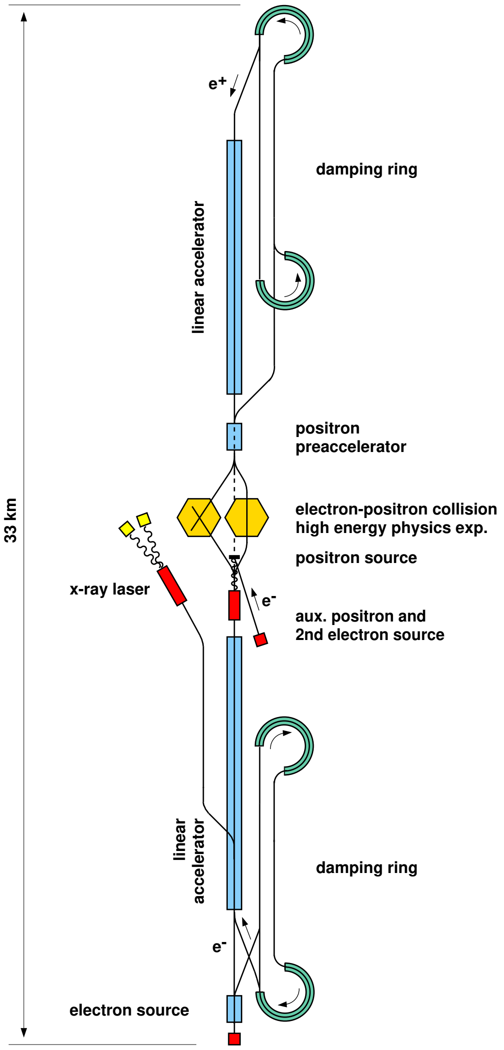

Figure 1: *Sketch of the overall layout of TESLA.*

The basic parameters of TESLA are:

$\sqrt{s}$	TeV	0.5
gradient	MeV/m	23.4
Luminosity	$10^{34}\text{cm}^{-2}\text{s}^{-1}$	3.4
train/s		5
beam pulse length	μs	950
bunches/train		2820
bunch spasing	ns	337
charge per bunch		$2{\cdot}10^{10}$
beam size, σ_x	nm	553
beam size, σ_y	nm	5
bunch length, σ_z	mm	0.3

1.2 Luminosity calorimeter LCAL

The instrumentation of the forward region of the detector is important for the measurement of the luminosity and for the search of new physics signatures. Therefore the calorimetric coverage at small polar angles is completed by two devices in the very forward region on both sides of the interaction point, the low angle tagger, LAT, and the luminosity calorimeter, LCAL. In Figure 2 the placement of the two calorimeters in the detector structure is shown.

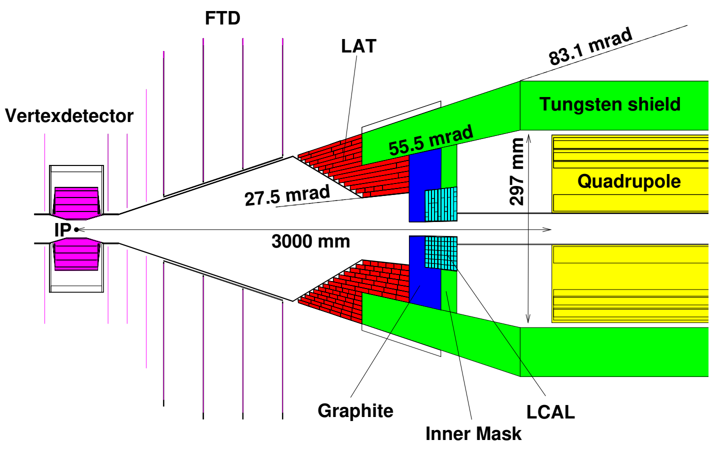

Figure 2: *Design of the forward angle calorimeters. Note the different horizontal and vertical scales.*

The LCAL, which serves both as a fast luminosity monitor and as a low angle calorimeter will be placed at a distance of 220 cm on both sides of the interaction point, covering an angular range between 5.5 and 27.5 mrad. For the gross luminosity determination, the detector will measure the amount of beam induced background particles. As a calorimeter, the LCAL will be used to measure showers originating from electrons and photons.

2 Analysis

2.1 The Problem

The LCAL is exposed to an enormous flux of electrons and positrons originating from beam-beam effects in the interaction region. The e^+e^-pairs stem from conversion of beamstrahlung photons in the high electromagnetic field of the colliding bunches. Their energies are in the range between a few MeV and a few GeV. The number of pairs per bunch crossing is about 130000. The sum of the energies amounts to about 360 TeV.

In this background is necessary to detect high energy electrons, positrons and photons. Electrons and positrons are expected to be produced copiously via Bhabha scattering and two-photon processes. The cross section of Bhabha scattering depends on the polar angle of the particle as $1/\Theta^3$, *i.e.* most of these particles hit the detector in the innermost part. The same behaviour is, qualitatively, expected for two-photon processes and for photons from initial state bremsstrahlung.

If a high energetic electron hits the calorimeter, part of the shower leaks in longitudional and transverse directions. My task was to estimate this leakage, depending on the angle and the energy of the electron.

2.2 Detector simulation

The simulation was done using the program BRAHMS. BRAHMS is a GEANT 3-based software package allowing the detailed simulation of a detector for the TESLA linear collider.

The simulation was made for several angles between 5 and 28 mrad and for energies of 100, 300 and 500 GeV. Two detector types are considered: a scintillator $PbWO_4$ calorimeter and a diamond-tungsten sampling calorimeter. The geometry and granularity of both detector types is given in tabble 1.

Geometry :	
Distance between calorimeter front and IP	220 cm
Internal radius of the calorimeter	12 mm
External radius of the calorimeter	62 mm
Lenght	20 cm
Granularity of the scintillator calorimeter:	
Material	$PbWO_4$
Number of layers in z-direction	50
Thickness of layers	4 mm
Number of radially sectors	50
Number of azimuthally sectors	100
Granularity of sampling detector:	
Material	W/C
Number of layers in z-direction	63
Thickness of layers	2.7 mm/0.5 mm
Number of radially sectors	7
Number of azimuthally sectors	24

Table 1: *The geometry and granularity of LCAL used in the simulation.*

2.3 Results

2.3.1 Scintillator calorimeter

The depence of the energy deposition as function of the coordinate along the beam (longitudinal distribution) is shown in Figures 3 and 4 for electrons of 100 GeV and 500 GeV energy, respectively. The shape of the central calorimeter regions are very similar, the maximum of the deposition is reached at about $0.4\times$ calorimeter length and the longitudinal leakage is small. At the lower side of the polar angle the particles hit the calorimeter not in the front face but in a deeper layer, hence the shower development starts deeper in the calorimeter and the leakage becomes large. At large polar angles the maximum of the shower is shifted to the front side of the calorimeter, mainly due to tranverse shower leakage. This behaviour is more pronounced at larger energy. The dependence of the energy leakage on the polar angle Θ is shown in Figures 5 and 6 for electrons of 100 GeV and 500 GeV energy, respectively. The leakage is of about 5% in the central regions of the calorimeter and growths when the polar angle of the particle approaches the inner or outer end of the calorimeter. There is no strong energy dependence visible.

2.3.2 Sampling calorimeter

Only the energy depositions in the diamond layers are considered, since tungsten is an absorber only. The depence of the energy deposition as function of the coordinate along the beam (longitudinal distribution) is shown in Figures 7 and 8 for electrons of 100GeVand 500GeVenergy, respectively. The shape of the central calorimeter regions are very similar, the maximum of the deposition is reached at about $0.25\times$ calorimeter length. There is almost no longitudinal leakage. At the lower and upper bounds of the polar angle the behaviour is similar to the scintillator calorimeter.

The dependence of the energy leakage on the polar angle Θ is shown in Figures 9 and 10 for electrons of 100GeVand 500GeVenergy, respectively. The leakage is, due to the tungsten absorber, of about 86% in the central regions of the calorimeter and growths when the polar angle of the particle approaches the inner or outer end of the calorimeter. The region of almost constant leakage is wider than in the case of the scintillator calorimeter. There is no strong energy dependence visible.

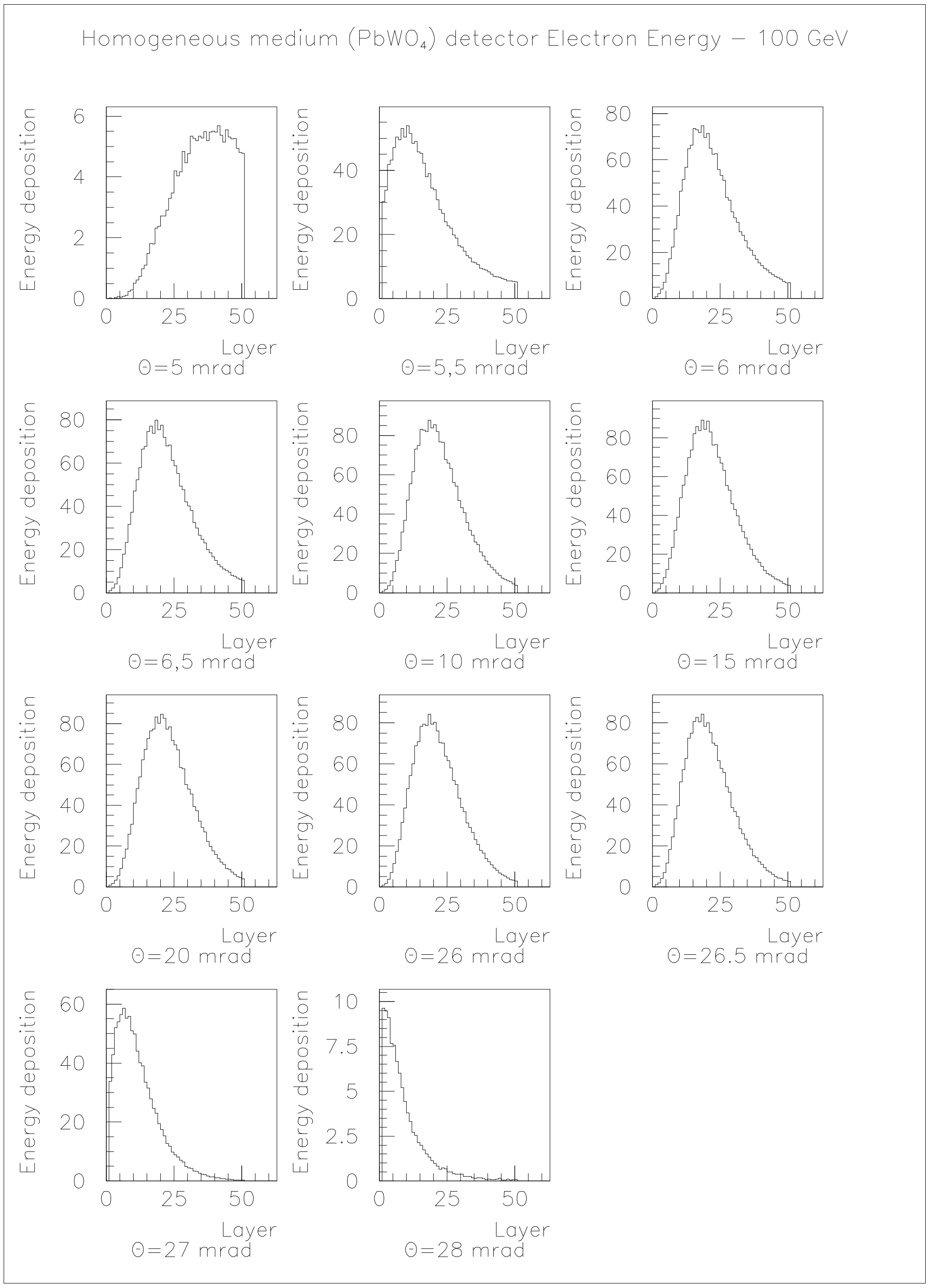

Figure 3: *Energy depositions per layer induced by 100 GeV e^- in $PbWO_4$ for different Θ. Each plot contains the sum of 20 events. The energy deposition of a single electron in GeV is received by division of 20.*

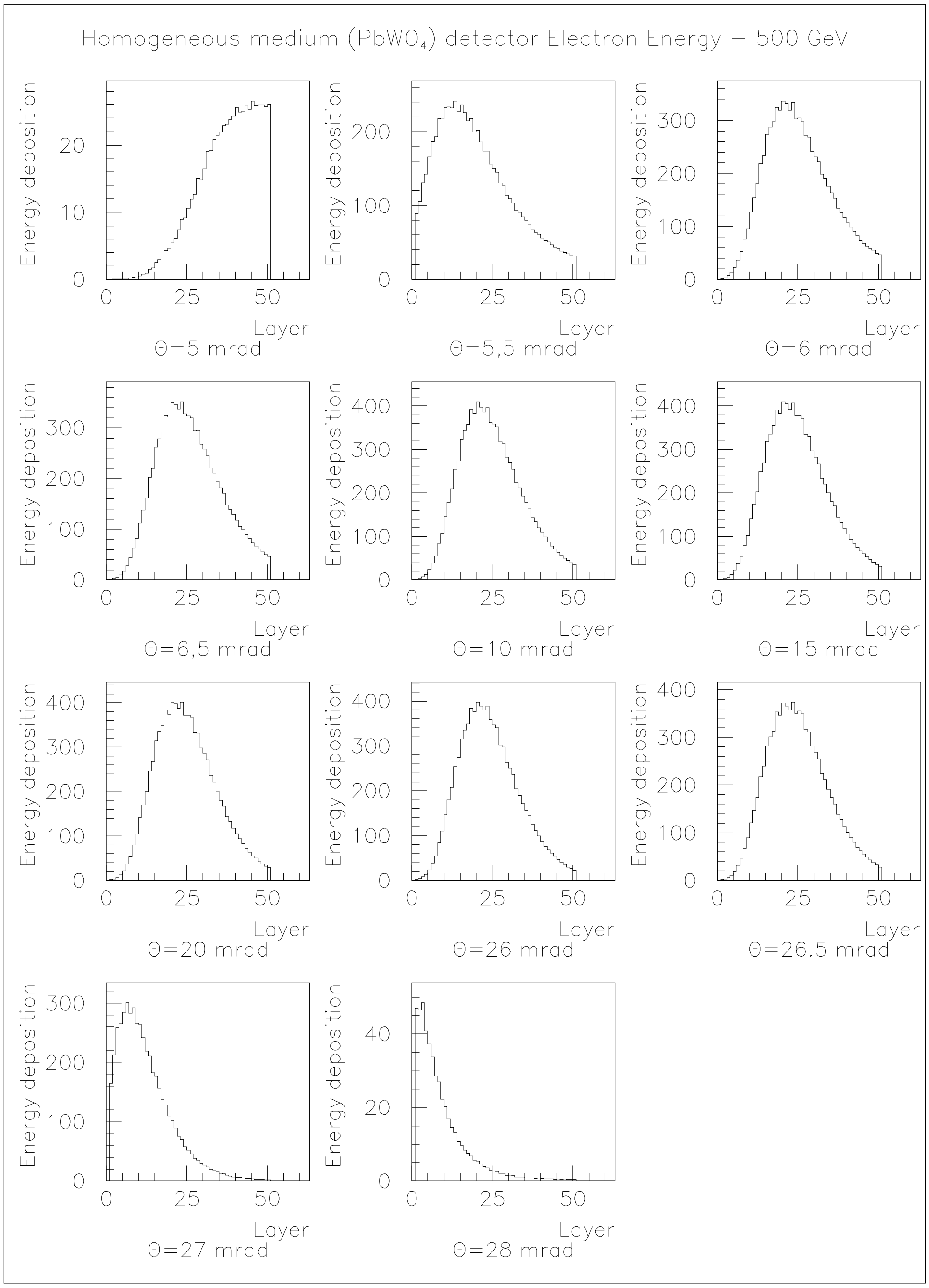

Figure 4: *Energy depositions per layer induced by 500 GeV e^- in $PbWO_4$ for different Θ. Each plot contains the sum of 20 events. The energy deposition of a single electron in GeV is received by division of 20.*

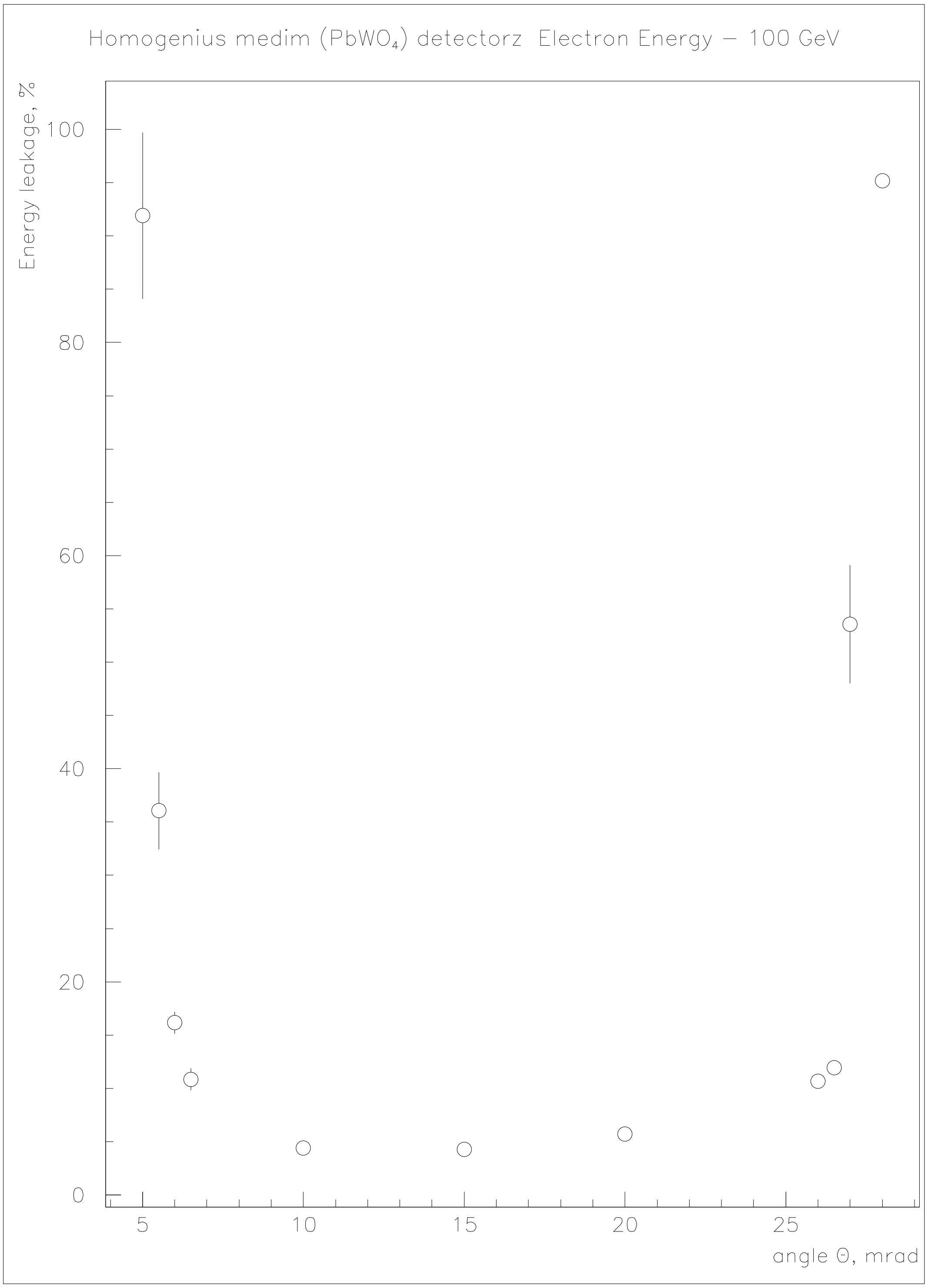

Figure 5: *Dependence of shower energy leakage of 100 GeV e^- in the $PbWO_4$ calorimeter on* Θ.

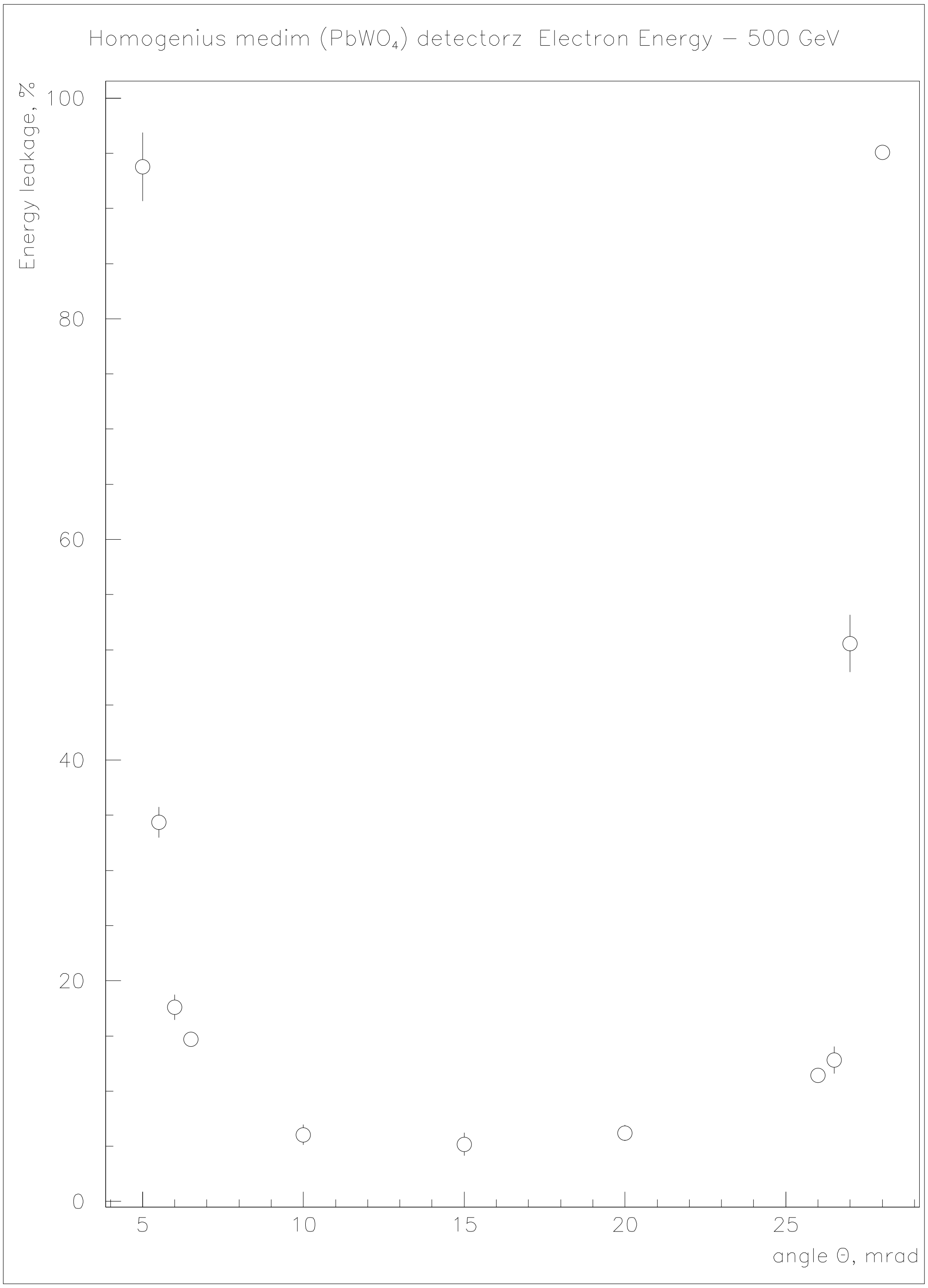

Figure 6: *Dependence of shower energy leakage of 100 GeV e^- in the $PbWO_4$ calorimeter on Θ.*

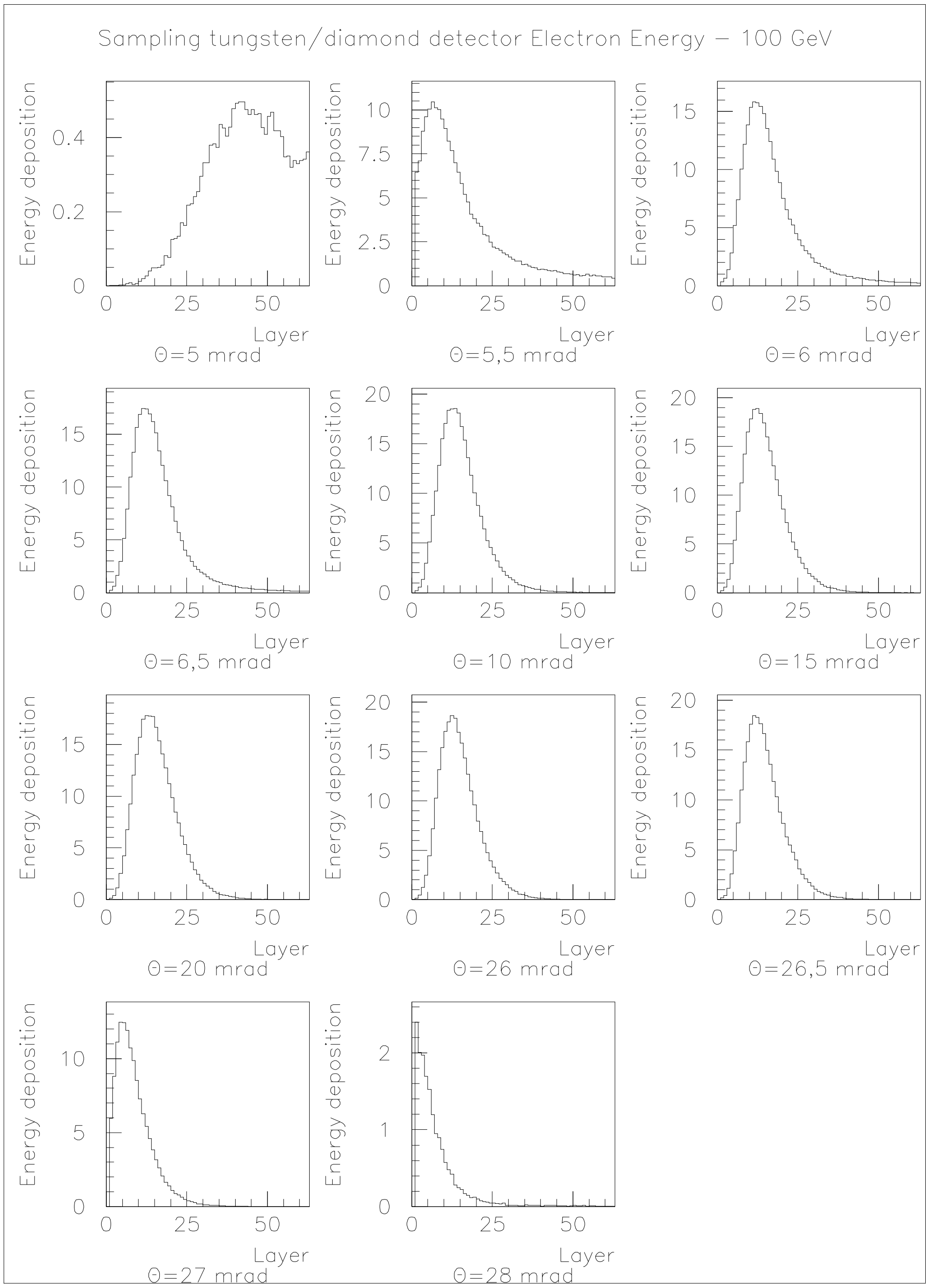

Figure 7: *Energy depositions per layer induced by 100 GeV e^- in the sampling calorimeter for different Θ. Each plot contains the sum of 20 events. The energy deposition of a single electron in GeV is received by division of 20.*

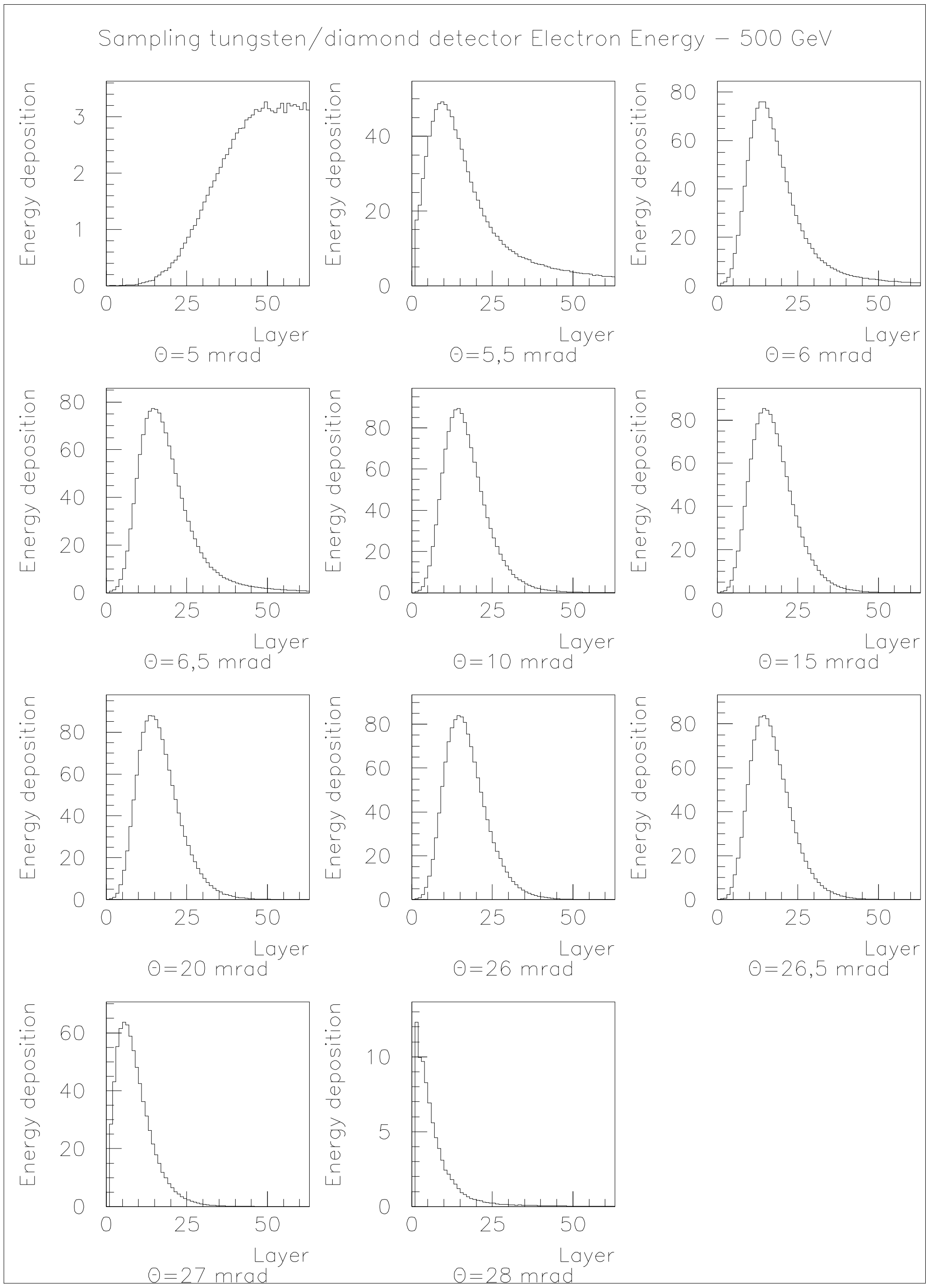

Figure 8: *Energy depositions per layer induced by 100 GeV e^- in the sampling calorimeter for different Θ. Each plot contains the sum of 20 events. The energy deposition of a single electron in GeV is received by division of 20.*

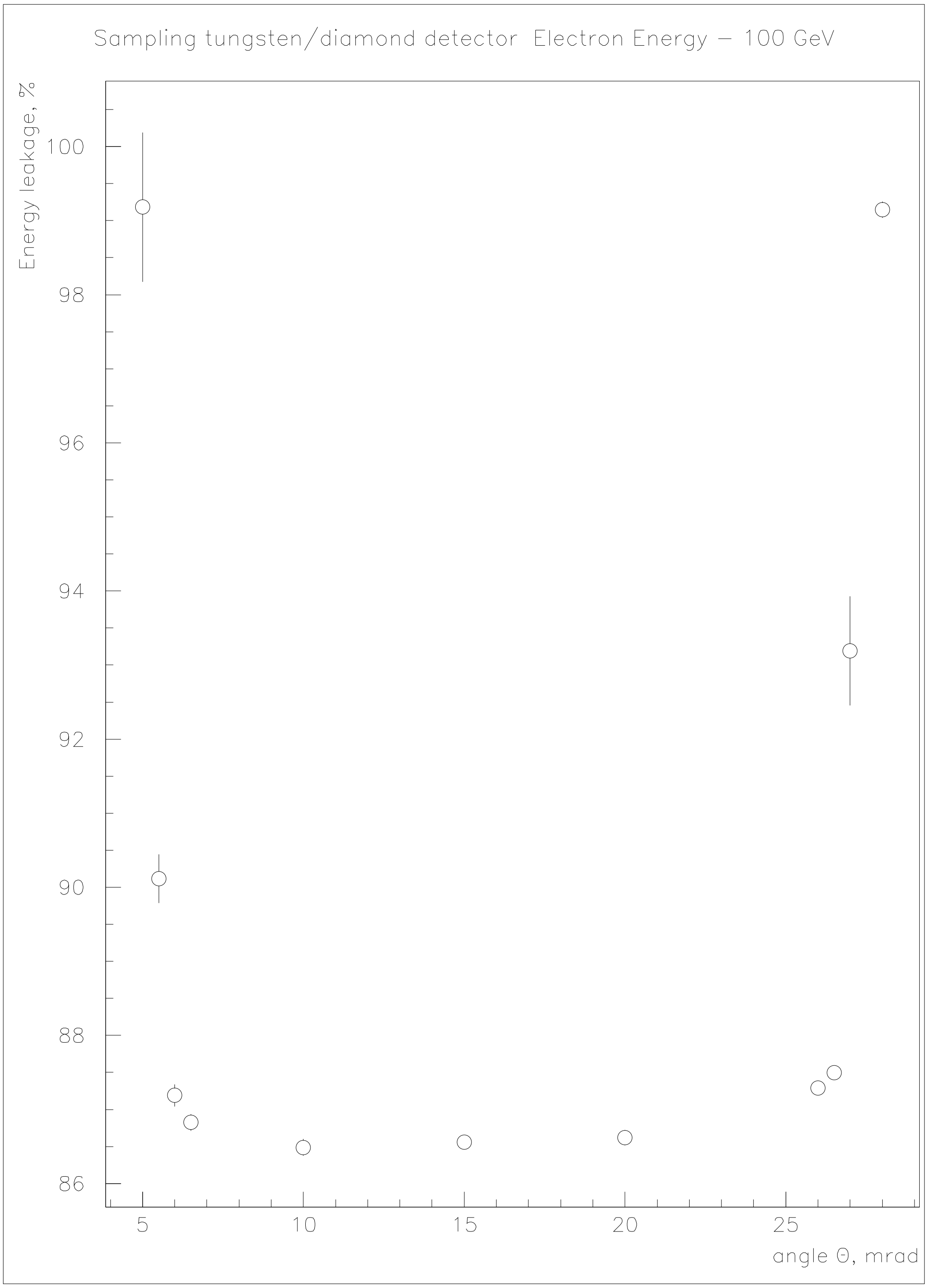

Figure 9: *Dependence of shower energy leakage of 100 GeV e^- in the sampling calorimeter on* Θ*.*

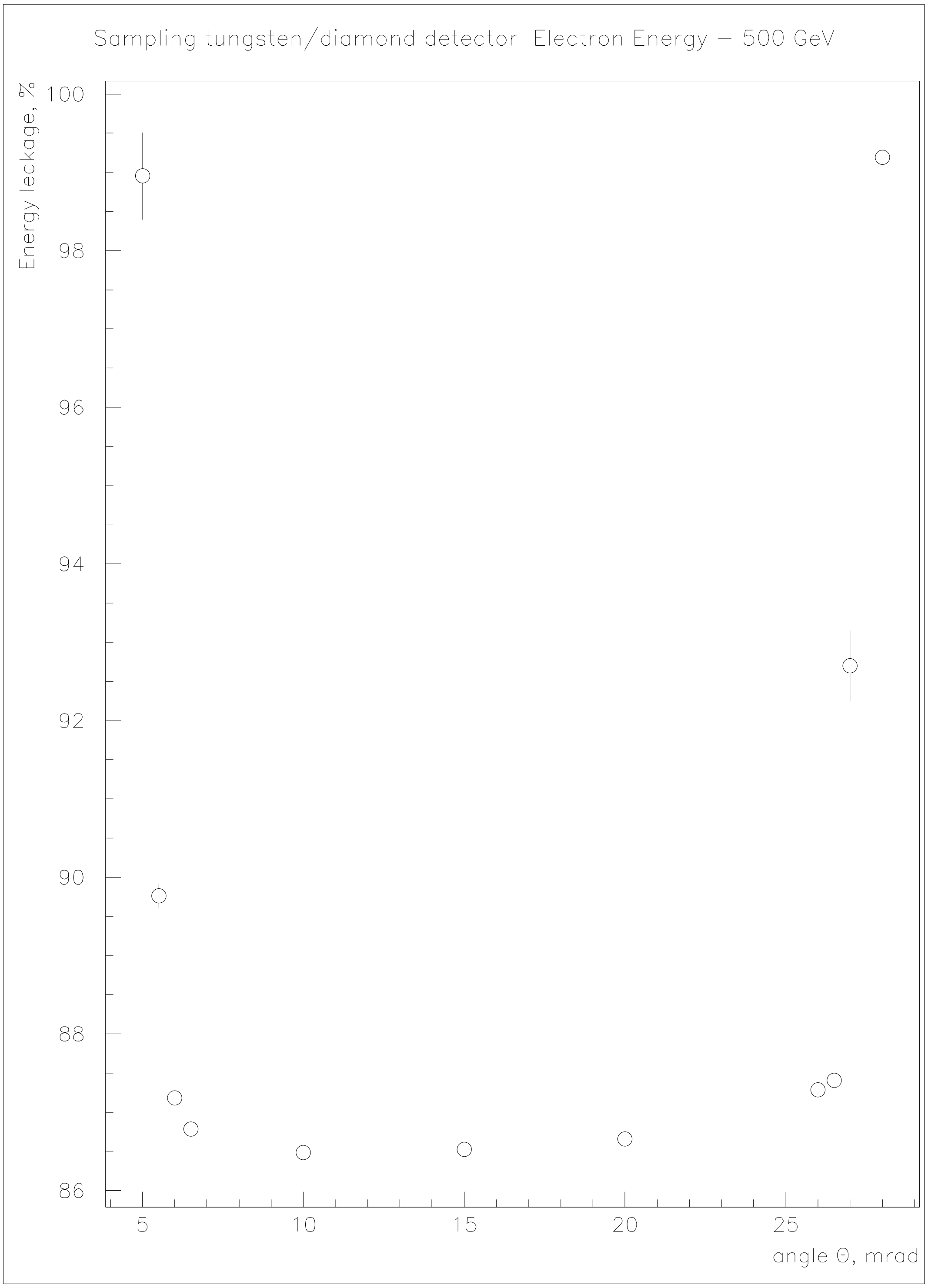

Figure 10: *Dependence of shower energy leakage of 500 GeV* e^- *in the sampling calorimeter on* Θ*.*